Parasitol Res (2008) 102:577–585
DOI 10.1007/s00436-007-0791-5

ORIGINAL PAPER

Inducible nitric oxide synthase inhibition influenced granuloma formation with suppressed collagen expression in myositis caused by *Toxocara canis* in mice

Su-Mei Lin · Chien-Wei Liao · Yun-Ho Lin · Chin-Cheng Lee · Ting-Chang Kao · Chia-Kwung Fan

Received: 26 August 2007 / Accepted: 30 October 2007 / Published online: 22 November 2007

Abstract The role of nitric oxide (NO) in granuloma pathology is largely unclear to date. We investigated the role of NO in fibrotic granuloma development in the musculature of mice infected with *Toxocara canis* from 1 day (dpi) to 8 weeks post-infection (wpi) using the NO synthase (NOS) inhibitors, L-NIL (l-N^6-1-iminoethyl lysine). In infected mice, elevated serum NO concentrations were seen at 1 dpi (204.1±0.2 μM) and 1 wpi (145.1±0.2 μM); it declined drastically from 4 wpi onwards (57.0±0.1 μM). In L-NIL-treated mice, the NO concentration was drastically reduced from 15% during 1 wpi; thereafter, it was restored to almost half that in infected mice. Inducible NOS expression was enhanced in infected and L-NIL-treated mice at 4 wpi but declined at 8 wpi as assessed by immunohistochemistry. L-NIL treatment resulted in large, irregularly shaped granulomas with suppressed collagen contents at 4 wpi but not at 8 wpi. The suppressed collagen contents might have been related to decreased serum NO and Th2-type cytokine of interleukin-4 but not Th1-type cytokine of interferon-γ expression.

S.-M. Lin · C.-C. Lee
Department of Pathology and Laboratory Medicine,
Shin-Kong Wu Ho-Su Memorial Hospital,
Taipei, Taiwan

C.-W. Liao · T.-C. Kao · C.-K. Fan
Department of Parasitology,
Taipei Medical University College of Medicine,
Taipei, Taiwan

Y.-H. Lin · C.-C. Lee
Department of Pathology,
Taipei Medical University College of Medicine,
Taipei, Taiwan

T.-C. Kao · C.-K. Fan (✉)
Graduate Institute of Medical Sciences,
Taipei Medical University College of Medicine,
Taipei, Taiwan
e-mail: tedfan@tmu.edu.tw

Introduction

A granulomatous inflammatory response is the hallmark of a large number of human and animal diseases, including schistosomiasis, tuberculosis, and toxocariasis (Kayes and Oaks 1978; Stavitsky 2004; Lousada et al. 2006). Activated cells within granulomas liberate their products, which might impact dynamic characteristics to this kind of lesion, and nitric oxide (NO) is one of the mediators secreted by cells, which organize the granulomatous lesion (Kreuger et al. 1998). In mammalian cells, NO is formed from L-arginine by the enzyme, NO synthase (NOS, EC1.14.13.39). The family of NOS isoforms falls into two dominant categories: a constitutive low-output form [endothelial NOS (eNOS) and neuronal NOS (nNOS)] and a cytokine-inducible high-output form (iNOS). It has been recognized that CD_4^+ Th1-associated cytokines and bacterial products such as lipopolysaccharide can activate iNOS to produce high levels of NO that may play critical roles in host defense and pathological damage to host tissues (James 1995). Many studies have analyzed the protective role of NO in host defense against Th1-inducing protozoan infections, e.g., *Plasmodium falciparum*, as well as Th2-stimulating helminthic infections, e.g., *Schistosoma japonicum* (James 1995).

Toxocara canis is an intestinal nematode of canines, and its embryonated eggs are infectious to both final and paratenic hosts including humans and rodents (Kayes 2006). Clinical human toxocariasis cases associated with pyomyositis have been reported (Rayes et al. 2000). Several

studies have indicated that *T. canis* larvae might elicit varying degrees of granulomatous inflammation in internal organs including the musculature of mice (Fan et al. 2003; Kayes 2006). In addition, constant activation of the Th2-type immune response in experimental toxocariasis might drive these lesions to develop into fibrotic granulomas with an extensive extracellular matrix, e.g., collagen accumulation through modulation of fibrosis-related cytokines, especially of transforming growth factor-β1 (TGF-β1) that is harmfully destructive to these organs (Blobe et al. 2000; Cuellar et al. 2001; Fan et al. 2003; Kayes 2006).

Nevertheless, somatic *T. canis* L2 antigens are reported to be capable of stimulating the production of NO by rat alveolar macrophages through upregulation of iNOS in vitro (Espinoza et al. 2002a, b), and our previous study also indicated that infiltrated leukocytes expressing iNOS likely play an important role in the pathogenesis of granulomatous hepatitis caused by *T. canis* in mice (Fan et al. 2004a, b). However, the underlying mechanisms of how iNOS and/or NO exert their protective or destructive effects, e.g., fibrotic granuloma formation in tissue in vivo, remain unclear.

Our present studies indicated that iNOS inhibitions influence musculature granuloma formation by suppression of collagen expression as proposed due to decreased serum NO and interleukin-4 (IL-4), but not interferon-γ (IFN-γ), concentrations in mice infected with *T. canis*.

Materials and methods

Egg culture and the experiment protocol

Egg culture and the inoculation protocol were as described in our previous study (Fan et al. 2003). Briefly, female worms were dissected, and the anterior one third of the uterus was stirred in 10 ml of a 1% sodium hypochlorite solution and incubated for 5 min at room temperature; thereafter, distilled water was added to bring the volume up to 20 ml. The mixture was then filtered through two layers of gauze to remove large tissue debris, and the resulting material was centrifuged for 5 min at 2,000×*g*. The supernatant was discarded, and the pellet was washed twice with distilled water and once with 2% formalin. The eggs were resuspended in 2% formalin and placed in a 250-ml Erlenmeyer flask, to which additional 2% formalin was added to bring the liquid level to approximately 1 cm deep. The flask was covered with parafilm (American National Can™, Greenwich, CT, USA) and incubated at room temperature for 8~9 weeks with gentle weekly agitation; thereafter, they were stored at 4°C until use. Eggs were washed with water to remove the formalin before use.

Female ICR mice aged 6~8 weeks were obtained from the Center for Experimental Animals, Academia Sinica, Taipei, Taiwan. Mice were housed in the animal facility of Taipei Medical University and maintained on commercial pellet food and water ad libitum. Viability of the *T. canis* embryonated eggs was assessed by the light stimulation method before use (O'Lorcain 1995). Each mouse was infected with about 250 *T. canis* embryonated eggs in 100 μl of water by oral intubation (Fan et al. 2003).

Infected mice were deeply anesthetized with ether and killed by heart puncture at 1 day (dpi) and 1, 4, and 8 weeks post-infection (wpi), respectively. On each date, three infected mice and two age-matched uninfected mice were killed for serum collection and muscle processing. Serum was tested for either the presence of total nitrite derived from NO or cytokines including IL-4 and IFN-γ. Muscle tissue from each mouse was processed for the histological study.

All animal experiments were carried out in accordance with institutional *Policies and Guidelines for the Care and Use of Laboratory Animals of Taipei Medical University*, and all efforts were made to minimize animal suffering.

Treatment with NOS inhibitor

A selective iNOS inhibitor, l-N^6-(1-iminoethyl)-lysine (L-NIL; Sigma Chemical Co., St. Louis, MO, USA; Moore et al. 1994) was used, and it was administered according to the method described by Gabbai et al. (1997). Before treatment, the effects of 30 and 50 μg/ml L-NIL on inhibiting NO production at 1 dpi were pre-screened, and 50 μg/ml L-NIL was found to exhibit better effects at decreasing NO concentrations (data not shown). Thus, 50 μg/ml L-NIL was used and mixed with acidified drinking water, while normal tap water was provided to the control groups of uninfected mice. Treatment commenced 1 day after the mice were inoculated with the eggs. Water bottles were changed every other day until the end of the experiment. The amount of drinking water consumed was monitored during the course of the experiment. No difference in water intake was found between the treated and control groups of mice.

Serum nitrite determinations

After reducing the nitrate to nitrite with nitrate reductase, nitrite concentrations were indirectly measured by a quantitative colorimetric assay using the Griess reagent system (Promega, Madison, WI, USA; Fan et al. 2004a, b). This method had a sensitivity of up to 2.5 μM if low nitrite is present. Briefly, 50 μl of freshly prepared Griess reagent (1% sulfanilamide, 0.1% naphthylethylene diamide dihydrochloride, and 2.5% ortho-phosphoric acid) was added to 50-μl aliquots of serum and incubated at room temperature. Duplicate tests were run on each test sample. After 10 min,

the absorbance at 540 nm was determined in individual wells with an automated spectrophotometer (Molecular Devices, Vmax®, Sunnyvale, CA, USA). The nitrite concentration in samples was calculated with reference to a sodium nitrite standard curve.

Immune responses assessed by ELISA

The serum cytokines investigated were IL-4 and IFN-γ. Levels of production were determined by a sandwich enzyme-linked immunosorbent assay (ELISA) using commercially available reagents (R&D Systems, Minneapolis, MN, USA). When the level exceeded the detection limit, five- or tenfold dilutions were used. Cytokine levels in the serum were assessed in duplicate and averaged according to manufactory's instructions.

Histopathological changes and collagen distribution

The musculature obtained from the neck of each mouse was fixed separately in 10% neutral-buffered formalin for at least 24 h and embedded in paraffin for pathological and immunohistochemical studies. Several serial sections were cut at a 5-μm thickness for each muscle tissue from each mouse. Paraffin was removed by heating the sections for 1 h at 65°C. These sections were dewaxed by washing three times for 5 min each in xylene, then rehydrated through 100, 95, and 80% ethanol for 5 min each, and finally rinsed with distilled water. After staining with hematoxylin and eosin (H&E), pathological changes were examined under a light microscope. In addition, muscle sections were also processed for Masson–Trichrome (M&T) staining to assess the collagen distribution in the injured areas (Lopez et al. 2006).

Immunohistochemical detection of iNOS expression

Muscle sections were deparaffinized by incubation at 58°C for 40 min, followed by immersion in xylene and then rehydration through descending ethanol gradients before further processing. The method for immunohistochemical detection of iNOS was as described in our previous study (Fan et al. 2004a, b). Briefly, endogenous peroxidase activity was blocked with 3% hydrogen peroxide (Merck, Taufkirchen, Germany). The tissue section slides were submerged in 10 mM sodium citrate buffer at pH 6.0, and heated in an 830-W microwave oven (Sunpentown, Ciba, Japan) for at least 5 min to retrieve the antigens. To reduce the background staining, an avidin/biotin blocking kit (SP2001, Vector, Burlingame, CA, USA) was employed to block endogenous avidin/biotin activity in the muscle tissue. To eliminate nonspecific staining, Fc receptors were blocked with diluted normal goat serum (X0907, Dako, Carpinteria, CA, USA) for 30 min at room temperature in a humid chamber. Sections were then incubated for at least 12 h at 4°C with a rabbit anti-mouse iNOS polyclonal antibody (cat. no. 482728, EMD Biosciences, San Diego, CA, USA) diluted (at 1:500) in phosphate-buffered saline; thereafter, sections were washed with 0.05% Tween 20-Tris–HCl buffer three times for 5 min each. A set of immunohistochemical detection kits (K4003, Dako) was employed to detect iNOS-expressing cells, by incubation with the horseradish peroxidase-conjugated goat anti-rabbit antibody for 40 min at room temperature. The presence of peroxidase was detected with the chromogen 3,3-diaminobenzidine (K3468, Dako), which resulted in a brown color. Sections were counterstained with Gill's hematoxylin (H3401, Vector), dehydrated, and mounted with mounting medium (H5000, Neomarkers, Fremont, CA, USA). To confirm the validity of the staining results, a human tonsil section was used as a positive control (Fan et al. 2004a, b). To ascertain the specificity of the staining, positive control sections were treated as described above, but with omission of the primary antibody. In addition, human tonsil sections using normal rabbit serum as the primary antibody serving as negative controls were also included.

Quantification of iNOS-expressing cells, granuloma diameter, and collagen contents by computerized image analysis

Images for analysis were captured using a digital camera (Nikon, Coolpix 5700, Tokyo, Japan). To determine the granuloma diameter (mean of the longest length plus the width), each specimen slide was assessed microscopically under a low-power-field at 100× magnification by totally counting 10~15 granulomas per experimental group of infected (three mice/group) or L-NIL-treated mice (three mice/group). The mean percentages (%) of immunoreactive cells to anti-iNOS antibody or M&T-positive areas on each specimen slide were assessed microscopically under a high-power field (HPF) at 400× magnification by totally counting 15~20 or 20~30 fields of areas containing infiltrate or collagen per experimental group of infected mice (three mice/group), L-NIL-treated mice (three mice/group), or control group of uninfected mice (two mice/group) using an optical image analyzer (Image-Pro Plus 5.1, Media Cybernetics, Silver Spring, MD, USA). Values are expressed as the mean diameter of 10–15 granulomas, or the mean percentage (%) of iNOS-positive cells and M&T-positive areas calculated from 15~20 and 20~30 HPF areas ± the standard deviation of the mean (SD) of 10~15 granulomas, respectively. To confirm the results, most experiments were carried out at least twice.

Statistical analysis

Analysis of serum NO, cytokine concentrations, granuloma size, M&T-positive areas, and iNOS-positive cells was carried out with the Welch corrected unpaired *t* test or the non-parametric Mann–Whitney test. In all cases, $P<0.05$ was considered statistically significant. Statistical analysis was done using the software GraphPad Instant version 3.01 (GraphPad Software, San Diego, CA, USA).

Results

Reduced serum nitrite levels in L-NIL-treated groups of infected mice

The total serum NO level in infected mice quickly reached a peak of 204.1±0.2 μM at 1 dpi, which was almost seven times that of the control group of uninfected mice (29.5±0.1 μM; $P<0.001$). Thereafter, it gradually declined from 145.1±0.2 μM at 1 wpi to 38.4±0.1 μM at 8 wpi; however, it remained high at two to six times that of the control group of uninfected mice from 1 to 8 wpi (Fig. 1). In L-NIL-treated mice, the serum NO concentration (32.8±0.1 μM) drastically dropped to about 15.0% of the NO level in infected mice during 1 wpi; thereafter, it slightly increased to 40.5 and 53.6% of the NO level in infected mice at 4 wpi (23.1±0.3 μM) and 8 wpi (20.6±0.0 μM), respectively (Fig. 1). Nonetheless, the NO levels in L-NIL-treated mice remained higher than that of uninfected aged-matched control mice at 1 dpi, 1, and 8 wpi, respectively ($P<0.001$; Fig. 1).

L-NIL treatments alter the morphology of *T. canis* larvae-induced lesions

Lesions induced by *T. canis* larvae in the musculature of mice were characterized by varying sizes of intact granuloma with inflammatory cells including polymorphonuclear (PMN) leukocytes, epithelioid cells, and multinucleated giant cells at both 4 and 8 wpi (Figs. 2 and 3a). When the animals were treated with L-NIL, the architecture of the granulomatous lesions seemed to become more irregular and looser with necrotic debris than that seen in infected mice at 4 or 8 wpi (Figs. 2 and 3b). Moreover, a significant increase in the diameter of *T. canis*-induced granuloma in the musculature of L-NIL-treated mice was seen at both 4 and 8 wpi (Figs. 2, 3a and b, and 4a).

At 4 and 8 wpi, it was evident that the granuloma size in infected mice treated with L-NIL (466.8±65.6 or 428.7±54.6 μm; $P<0.001$) was larger than that in the infected group of mice (305.9±37.0 or 234.7±45.2 μm; Fig. 4a). Nevertheless, the granuloma size slightly decreased with time as observed from 4 to 8 wpi in both experimental groups of mice in the trial (Fig. 4a).

Decreased collagen deposition in granulomas influenced by NOS inhibition

In general, the pattern of collagen distribution was nearly identical among these three experimental groups of mice in the trial. Most of the collagen deposition was present in the outer rim of granulomas by 4 wpi (Fig. 2c,d). The staining intensity became more prominent and was predominantly deposited amid the granulomas as observed at 8 wpi in these three experimental groups of mice (Fig. 3c,d).

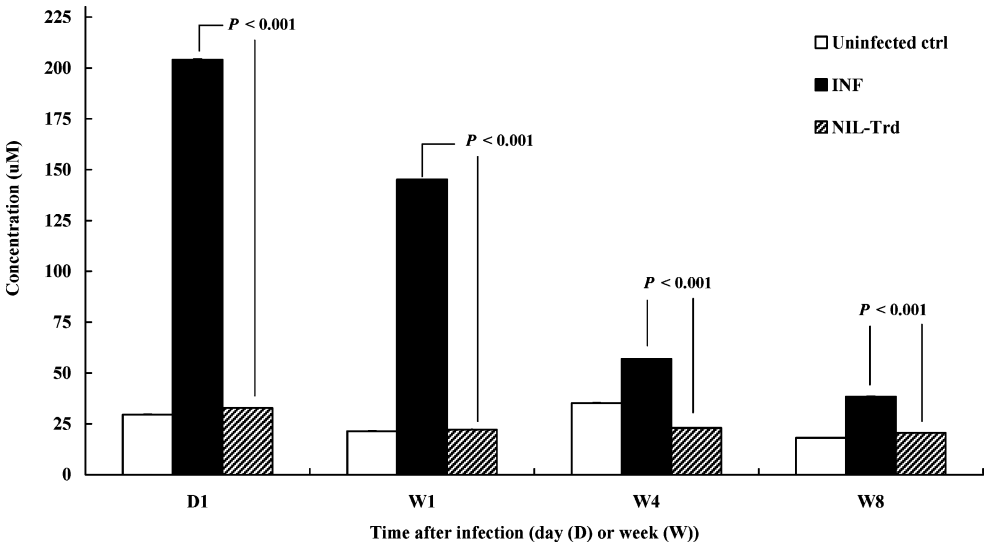

Fig. 1 Chronological changes in concentrations of serum nitrite calculated from *Toxocara canis*-infected mice (*INF*; $n=3$) and *T. canis*-infected mice treated with L-NIL (*L-NIL-Trd*; $n=3$), and uninfected control mice (*Uninfected ctrl*; $n=2$) from day (*D*) 1 to week (*W*) 8 post-infection

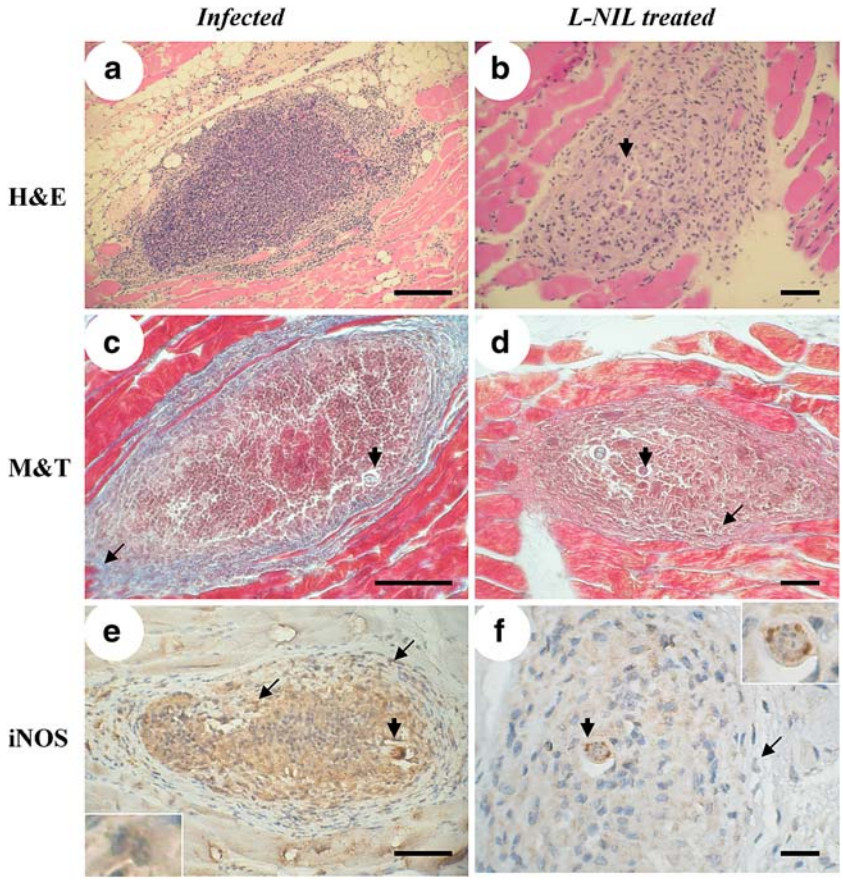

Fig. 2 Representative pathological changes, collagen distribution, and inducible nitric oxide synthase (*iNOS*) expressions in the musculature from mice infected with *Toxocara canis* with or without treatment with L-NIL at 4 weeks post-infection assessed by hematoxylin–eosin (H&E), Masson–Trichrome (*M&T*), and immunohistochemical (*IHC*) staining. H&E staining: Developing granuloma with intensive inflammatory infiltration in *T. canis*-infected mice (**a**), *T. canis*-infected mice treated with L-NIL (**b**). The *arrowhead* indicates a larval section. M&T staining: Abundant collagen deposition in granuloma in *T. canis*-infected mice (**c**), whereas suppressed collagen deposition was seen in *T. canis*-infected mice treated with L-NIL (**d**). The *arrow* indicates collagen, and the *arrowhead* indicates a larval section. IHC staining: Inflammatory cells with intensive iNOS expression in granuloma in *T. canis*-infected mice (**e**), whereas weak iNOS expression was seen in *T. canis*-infected mice treated with L-NIL (**f**). The *arrow* indicates iNOS-expressing infiltrated cells, and the *arrowhead* indicates a larval section. The *inserts* are higher magnifications of iNOS-expressing infiltrated cells and iNOS-like molecule detected in larvae in **e** and **f**, respectively. All bars=50 μm

Between both experimental groups as assessed at 4 wpi, a significant difference in collagen contents in granulomas was observed in L-NIL-treated mice (3.2±1.0%, $P<0.05$) compared to that in infected mice (5.7±1.9%; Fig. 4b). At 8 wpi, no significant difference in collagen contents between these two groups was found ($P>0.05$; Fig. 4b). Nevertheless, collagen significantly increased by 1.6- to3.4-fold as observed from 4 to 8 wpi in both experimental groups (Fig. 4b). No collagen deposition was found in the musculature of any uninfected age-control mice (data not shown).

Reduced iNOS expression in L-NIL-treated groups of infected mice

Localization of iNOS reactivity revealed that most of the infiltrating PMN leukocytes whether in the middle or at the rim of granulomas were positive for iNOS in both experimental groups of mice, whereas fainter intensity of iNOS staining in L-NIL-treated mice than that in infected mice was found at 4 and 8 wpi (Figs. 2 and 3e,f). Interestingly, strong iNOS-like molecule expression was also detected on the surface or body of larvae trapped in granulomas in both experimental groups of mice (Figs. 2 and 3e,f). The normal musculature was always negative for iNOS as seen in the infected mice, L-NIL-treated mice, and uninfected mice. Furthermore, negative controls showed no iNOS signal (data not shown).

Overall the highest iNOS expression was observed at 4 wpi, which then had declined by 8 wpi in both experimental groups of mice (Fig. 4c). The percentage of iNOS-positive inflammatory cells at 4 wpi in infected mice (31.2±3.7%) was higher than that in L-NIL-treated mice (18.6±5.4%) (Fig. 4c). At 8 wpi, no statistical difference

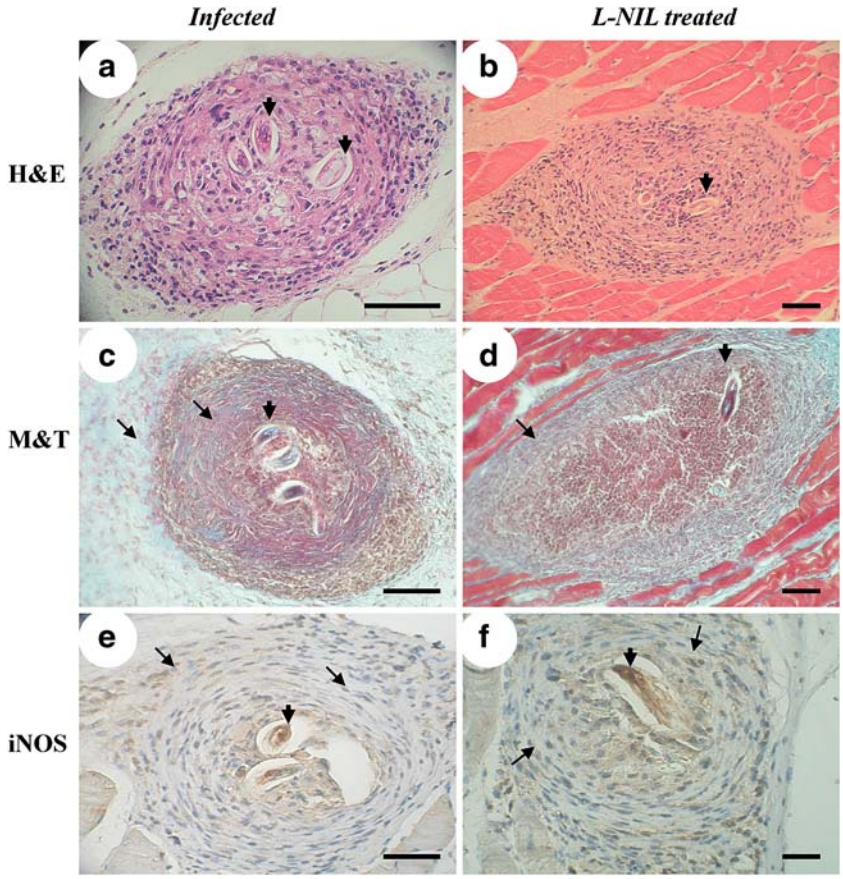

Fig. 3 Representative pathological changes, collagen distribution, and inducible nitric oxide synthase (*iNOS*) expressions in the musculature of mice infected with *Toxocara canis* with or without treatment with L-NIL at 8 weeks post-infection assessed by hematoxylin–eosin (*H&E*), Masson-Trichrome (*M&T*), and immunohistochemical (*IHC*) staining. H&E staining: Developed granuloma with trapped larvae in *T. canis*-infected mice (**a**) and *T. canis*-infected mice treated with L-NIL (**b**). The *arrowhead* indicates a larval section. M&T staining: Apparent collagen deposition in granuloma in *T. canis*-infected mice (**c**) and *T. canis*-infected mice treated with L-NIL (**d**). The *arrow* indicates collagen, and the *arrowhead* indicates a larval section. IHC staining: Inflammatory cells with moderate iNOS expression in granuloma in *T. canis*-infected mice (**e**), whereas weak iNOS expression was seen in *T. canis*-infected mice treated with L-NIL (**f**). The *arrow* indicates iNOS-expressing infiltrating cells, and the *arrowhead* indicates a larval section with iNOS-like expression. All bars=50 μm

was evident between infected mice (18.4±1.8%) and L-NIL-treated mice (16.5±4.4%; $P>0.05$; Fig. 4c).

Inhibition of iNOS did not materially affect the Th2 bias of the immune response to *T. canis* infection

A Th2-type response is commonly associated with IL-4, while IFN-γ is associated with a Th1-type one (Ansel et al. 2006). Overall, a significantly higher IL-4 concentration was found in infected mice and L-NIL-treated mice than in uninfected control mice in the trial; nevertheless, infected mice (132.68±6.73 and 185.72±19.97 pg/ml; $n=3$) exhibited a higher IL-4 concentration than that of L-NIL-treated mice (104.24±1.75 and 119.92±27.27 pg/ml; $n=3$) as seen at 1 and 4 wpi, respectively ($P < 0.05$; Fig. 4d). However, similarly high IL-4 concentrations were found between these two experimental groups of mice at 8 wpi (Fig. 4d). Regarding IFN-γ, no significant difference was found between infected ($n=3$) and L-NIL-treated mice ($n=3$) from 1 dpi to 8 wpi; in addition, no significant difference in IFN-γ concentration was found between any of these two experimental groups of mice and uninfected control mice (15.26±1.06 pg/ml; $n=8$) in the trial (Fig. 4e).

Discussion

Previous studies indicated that iNOS is clearly involved in a variety of inflammatory processes elicited by various microbial pathogens including parasites (James 1995; Kreuger et al. 1998; Stavitsky 2004; Lousada et al. 2006). Although several studies have indicated that iNOS exerts deleterious effects on the liver, brain, and lungs of *T. canis*-infected rodents (Fan et al. 2004a, b; Gargili et al. 2004)

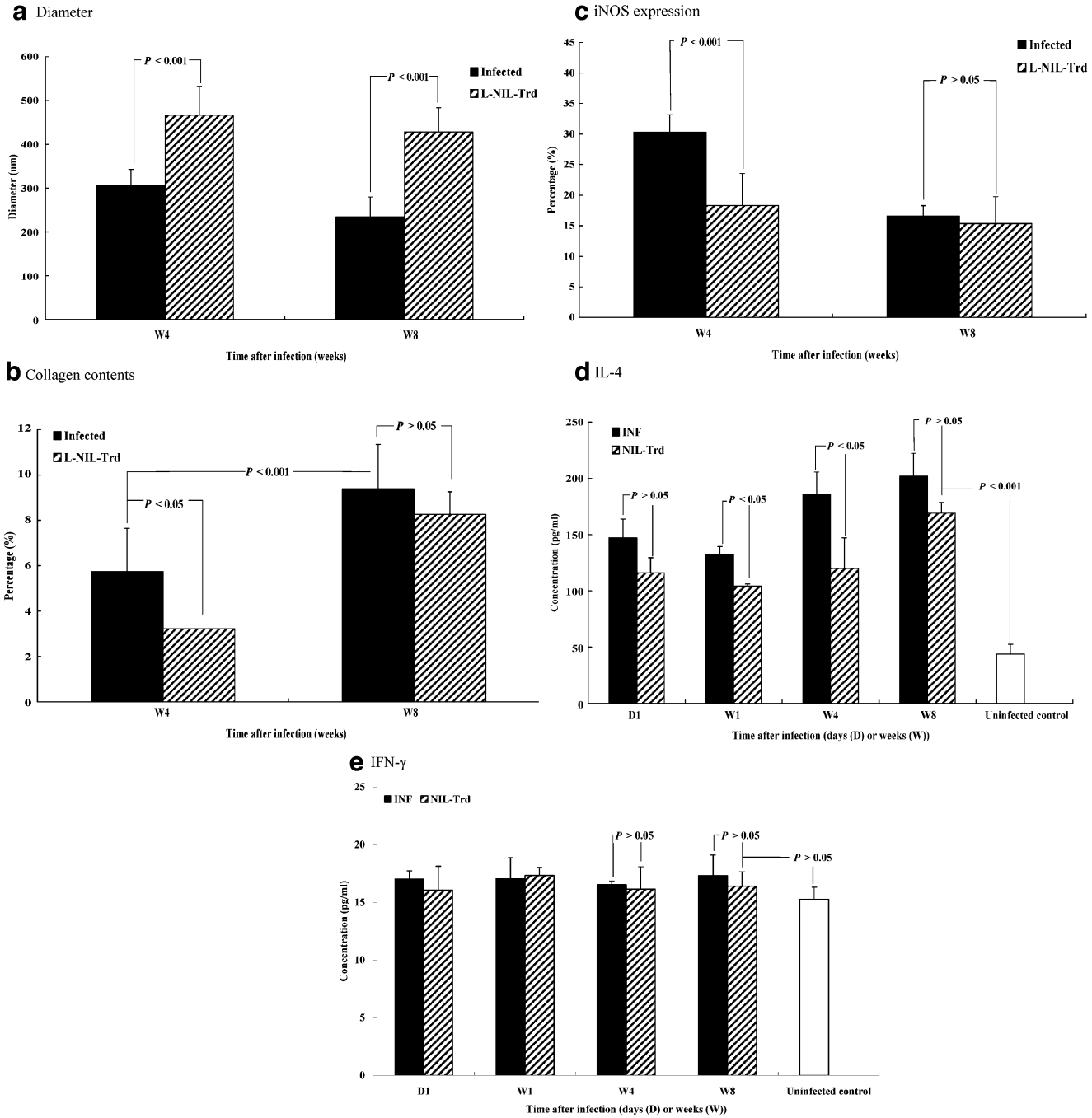

Fig. 4 Mean diameter (**a**) calculated from 10~15 granulomas at 100× magnification from nine slide specimens of *Toxocara canis*-infected mice (*Infected*; $n=3$) and *T. canis*-infected mice treated with L-NIL (*L-NIL-Trd*; $n=3$) at 4 and 8 weeks (*W*) post-infection, respectively. The mean percentage of collagen distribution (**b**) calculated from 20~30 HPFs of 10~15 granulomas at 400× magnification from nine slide specimens of *Toxocara canis*-infected mice (*Infected*; $n=3$) and *T. canis*-infected mice treated with L-NIL (*L-NIL-Trd*; $n=3$) at 4 and 8 weeks post-infection, respectively. The mean percentage of iNOS expression (**c**) calculated from 15~20 HPFs of 10~15 granulomas at 400x magnification from 9 slide specimens of *Toxocara canis*-infected mice (*Infected*; $n=3$) and *T. canis*-infected mice treated with L-NIL (*L-NIL-Trd*; $n=3$) at 4 and 8 weeks post-infection, respectively. The IL-4 (**d**) and IFN-γ (**e**) concentrations ± standard deviation (*SD*) calculated from pooled serum of *Toxocara canis*-infected mice (*Infected*; $n=3$), *T. canis*-infected mice treated with L-NIL (*L-NIL-Trd*; $n=3$), and uninfected control mice ($n=8$) from day 1 to week 8 post-infection

and inhibition of iNOS expression might diminish such damage caused by this enzyme (Espinoza et al. 2002a, b; Gargili et al. 2004; Demirci et al. 2006), there have been no studies of iNOS/NO's involvement in fibrotic granuloma formation in myositis elicited by *T. canis* in mice. In the present study, we investigated the role of iNOS/NO in granuloma formation in the musculature of *T. canis*-infected mice using the NOS inhibitors, L-NIL.

In the present study, vigorous serum NO production was detected at the beginning of infection at 1 dpi, which then declined drastically from 4 wpi onwards. This finding is basically similar to the kinetics of NO production reported in our previous study (Fan et al. 2004a, b) and studies on *S. japonicum* by Hirata et al. (2001). This result seems to explain why the rapid increase in NO production in the early infection is associated with an early inflammatory response against *T. canis* larval invasion; however, this free radical seemed likely to be useless in killing this parasite. Espinoza et al. (2002a, b) indicated that nitric oxide donors exerted no cytotoxic effect on the in vitro viability of *T. canis* larvae. The present study showed that L-NIL exhibited potent inhibitory effects on NO synthesis during *T. canis* infection. As iNOS, but not eNOS or nNOS, exerts potent effects on massive NO production during tissue damage/repair (Schwentker et al. 2002), it might be explained by L-NIL directly inactivating iNOS activity through altering heme residues at the active site thus leading to loss of the ability to catalyze the NOS substrate, L-arginine, to form large amounts of NO (Bryk and Wolff 1998).

In the present study, we investigated iNOS expressions in musculature granulomas at 4 and 8 wpi because no granulomatous lesions were found in musculature tissues in any of these two experimental groups of mice at 1 dpi or 1 wpi. When iNOS expression was detected by immunohistochemistry, the most vigorous iNOS expression was found in infected mice at 4 wpi when the granulomas were under-developed; 4 weeks later, it was markedly decreased when the granulomas had matured. However, very faint iNOS expression was found in infected mice treated with L-NIL at 4 wpi, which confirms that this chemical was effective in inhibiting iNOS expression. This result was also similar to those of studies of *S. japonicum* egg-induced granuloma formation in mouse liver treated by L-NIL (Hirata et al. 2001).

Interestingly, *T. canis* larvae per se seemed to have an iNOS-like molecule in their hypodermis and muscle, and this molecule did not seem to be influenced by L-NIL treatment as observed in Figs. 2 and 3f; this finding was also seen in larvae trapped in hepatic granulomas in our previous study (Fan et al. 2004a, b) and one by Demirci et al. (2006). Although it remains unclear why this iNOS-like molecule occurs in the hypodermis and muscle of *T. canis* larvae, it was proposed that this iNOS-like molecule might facilitate larval migration or adaptation in host tissues (Espinoza et al. 2002a, b; Demirci et al. 2006) because regardless of whether NO is released from either host cells or the parasite itself, it triggers blood vessel dilation (Torreilles 2001). Laboratory toxocariasis models have described how *T. canis* larvae are characterized by migration through the bloodstream until they reach their final niche inside the host, and this bloodstream migration is clearly facilitated by blood-vessel dilatation (Espinoza et al. 2002a, b). However, the assumption that larval NO might also be effective in larval migration requires further investigation (Demirci et al. 2006). Nevertheless, cross-reactivity between mammalian and nematode enzymes or a non-specific binding effect might also be possible.

The effect of NOS inhibition with suppressed collagen deposition was observed during granuloma formation with L-NIL treatments at 4 wpi. Many studies have indicated that iNOS and NO play a certain role in wound healing, which requires increased collagen synthesis and deposition through NO-mediated activation of various cytokines especially of TGF-β1 (Roberts and Sporn 1996; Cuellar et al. 2001; Schwentker et al. 2002). In both animal studies and in vitro, the link between NO and collagen deposition has been well described. In most studies, treatment with NO donors (Muscara et al. 2000), dietary L-arginine (Shi et al. 2000), or iNOS overexpression via gene therapy (Thornton et al. 1998) increased the collagen content of experimental wounds. Similarly, NOS inhibition was found to decrease collagen and granulation tissue formation in experimental burn and cutaneous wounds (Akcay et al. 2000). However, inflammatory cells expressing TGF-β1 provide indirect evidence that they play a certain role in collagen synthesis of fibrotic granuloma formation in the trial because inflammatory cells with apparent TGF-β1 expression infiltrating in granulomas in the submucosa of the small intestine were detected in *T. canis*-infected mice as described in our previous study (Fan et al. 2004a, b). Moreover, the suppression of collagen synthesis caused by iNOS inhibitor treatment at 4 wpi seemed to be a transitory phenomenon because collagen contents in inhibitor-treated mice were restored to levels nearly even with those in infected mice at 8 wpi. This might be explained by the Th2 response playing a certain role in promoting increased collagen synthesis in granuloma formation as proposed by modulation of arginase activity in metabolizing L-arginine, as significant IL-4 responses were still evident at 8 wpi in L-NIL-treated mice. It was indicated that arginase activity, which is highly regulated by Th2 immune response, is capable of metabolizing L-arginine to promote collagen production (Hesse et al. 2001).

The effect of NOS inhibition on granulomas appeared to vary with the eliciting agents and experimental conditions. A significant increase in size was also shown in *S. japonicum* egg implantation in the liver after L-NIL treatments (Hirata et al. 2001) and in PPD-induced pulmonary granuloma formation (Hogaboam et al. 1998). However, regulation by the Th2 immune response appeared to be involved in the present findings, which suggests a complex granuloma regulatory process.

Acknowledgements This study was sponsored by the Shin Kong Wu Ho-Su Memorial Hospital (SKH-TMU-93–10). We are grateful to Mr. Chamberlin D for revision and edition of our manuscript.

References

Akcay MN, Ozcan O, Gundogdu C, Akcay G, Balik A, Kose K, Oren D (2000) Effect of nitric oxide synthase inhibitor on experimentally induced burn wounds. J Trauma 49:327–330

Ansel KM, Djuretic I, Tanasa B, Rao A (2006) Regulation of Th2 differentiation and IL-4 locus accessibility. Ann Rev Immunol 24:607–656

Blobe GC, Schiemann WP, Lodish HF (2000) Role of transforming growth factor beta in human disease. New Eng J Med 342:1350–1358

Bryk R, Wolff DJ (1998) Mechanism of inducible nitric oxide synthase inactivation by aminoguanidine and L-N^6-(l-iminoethyl) lysine. Biochemistry 37:4844–4852

Cuellar C, Fenoy S, del-Aguila C, Guillen L (2001) Isotype-specific immune responses in murine experimental toxocariasis. Mem Inst Oswaldo Cruz 96:549–553

Demirci C, Gargili A, Kandil A, Cetinkaya H, Uyaner I, Boynuegri B, Gumustas MK (2006) Inhibition of inducible nitric oxide synthase in murine visceral larva migrans: effects on lung and liver damage. Chin J Physiol 49:326–334

Espinoza EY, Muro A, Martin MM, Casanueva P, Perez-Arellano JL (2002a) *Toxocara canis* antigens stimulate the production of nitric oxide and prostaglandin E2 by rat alveolar macrophages. Parasite Immunol 24:311–319

Espinoza EY, Perez-Arellano JL, Carranza C, Collia F, Muro A (2002b) In vivo inhibition of inducible nitric oxide synthase decreases lung injury induced by *Toxocara canis* in experimentally infected rats. Parasite Immunol 24:511–520

Fan CK, Lin YH, Du WY, Su KE (2003) Infectivity and pathogenicity of 14-month-cultured embryonated eggs of *Toxocara canis* in mice. Vet Parasitol 113:145–155

Fan CK, Hung CC, Lin YH, Li MS, Su KE (2004a) Enhanced expression of transforming growth factor-beta1 in inflammatory cells and secretory granules in Paneth cells in the small intestine of mice infected with *Toxocara canis*. Parasitol Res 94:397–404

Fan CK, Lin YH, Hung CC, Chang SF, Su KE (2004b) Enhanced inducible nitric oxide synthase expression and nitrotyrosine accumulation in experimental granulomatous hepatitis caused by *Toxocara canis* in mice. Parasite Immunol 26:273–281

Gabbai FB, Boggiano C, Peter T, Khang S, Archer C, Gold DP, Kelly CJ (1997) Inhibition of inducible nitric oxide synthase intensifies injury and functional deterioration in autoimmune interstitial nephritis. J Immunol 159:6266–6275

Gargili A, Demirci C, Kandil A, Cetinkaya H, Atukeren P, Gumustas MK (2004) In vivo inhibition of inducible nitric oxide and evaluation of the brain tissue damage induced by *Toxocara canis* larvae in experimentally infected mice. Chin J Physiol 47:189–196

Hesse M, Modolell M, La Flamme AC, Schito M, Fuentes JM, Cheever AW, Pearce EJ, Wynn TA (2001) Differential regulation of nitric oxide synthase-2 and arginase-1 by type 1/type 2 cytokines in vivo: granulomatous pathology is shaped by the pattern of L-arginine metabolism. J Immunol 167:6533–6544

Hirata M, Hirata K, Kage M, Zhang M, Hara T, Fukuma T (2001) Effect of nitric oxide synthase inhibition on *Schistosoma japonicum* egg-induced granuloma formation in the mouse liver. Parasite Immunol 23:281–289

Hogaboam CM, Gallinat CS, Bone-Larson C, Chensue SW, Lukacs NW, Strieter RM, Kunkel SL (1998) Collagen deposition in a non-fibrotic lung granuloma model after nitric oxide inhibition. Am J Pathol 153:1861–1972

James SL (1995) Role of nitric oxide in parasitic infections. Microbiol Rev 59:533–547

Kayes SG (2006) *Toxocara*, the enigmatic parasite. CABI Publishing, Cambridge

Kayes SG, Oaks JA (1978) Development of the granulomatous response in murine toxocariasis. Am J Pathol 93:277–294

Kreuger MR, Tames DR, Mariano M (1998) Expression of NO-synthase in cells of foreign-body and BCG-induced granulomata in mice: influence of L-NAME on the evolution of the lesion. Immunology 95:278–282

Lopez E, del Pozo V, Miguel T, Sastre B, Seoane C, Civantos E, Llanes E, Baeza ML, Palomino P, Cárdaba B, Gallardo S, Manzarbeitia F, Zubeldia JM, Lahoz C (2006) Inhibition of chronic airway inflammation and remodeling by galectin-3 gene therapy in a murine model. J Immunol 176:1943–1950

Lousada S, Florido M, Appelberg R (2006) Regulation of granuloma fibrosis by nitric oxide during *Mycobacterium avium* experimental infection. Int J Exp Pathol 87:307–315

Moore WM, Webber RK, Jerome GM, Tjoeng FS, Misko TP, Currie MG (1994) L-N^6-(1-iminoethyl) lysine, a selective inhibitor of inducible nitric oxide synthase. J Med Chem 37:3886–3888

Muscara MN, McKnight W, Asfaha S, Wallace JL (2000) Wound collagen deposition in rats: effects of an NO-NSAID and a selective COX-2 inhibitor. Br J Pharmacol 129:681–686

O'Lorcain P (1995) The effects of freezing on the viability of *Toxocara canis* and *T. cati* embryonated eggs. J Helminthol 69:169–171

Rayes AA, Nobre V, Teixeira DM, Serufo JC, Filho GB, Antunes CM, Lambertucci JR (2000) Tropical pyomyositis and human toxocariasis: a clinical and experimental study. Am J Med 109:422–425

Roberts AB, Sporn MB (1996) The Molecular and Cellular Biology of Wound Healing: transforming growth factor-β. Plenum, New York

Schwentker A, Vodovotz Y, Weller R, Billiar TR (2002) Nitric oxide and wound repair: role of cytokines. Nitric Oxide 7:1–10

Shi HP, Efron DT, Most D, Tantry US, Barbul A (2000) Supplemental dietary arginine enhances wound healing in normal but not inducible nitric oxide synthase knockout mice. Surgery 128:374–378

Stavitsky AB (2004) Regulation of granulomatous inflammation in experimental models of schistosomiasis. Infect Immun 72:1–12

Thornton FJ, Schaffer MR, Witte MB, Moldawer LL, MacKay SL, Abouhamze A, Tannahill CL, Barbul A (1998) Enhanced collagen accumulation following direct transfection of the inducible nitric oxide synthase gene in cutaneous wounds. Biochem Biophys Res Commun 246:654–659

Torreilles J (2001) Nitric oxide: one of the more conserved and widespread signaling molecules. Front Biosci 6:1161–1172